Trajectory generation for road vehicle obstacle avoidance using convex optimization

G P Bevan[1,2]*, **H Gollee**[2], and **J O'Reilly**[2]
[1]School of Engineering and Computing, Glasgow Caledonian University, Glasgow, UK
[2]Centre for Systems and Control, Faculty of Engineering, University of Glasgow, Glasgow, UK

The manuscript was received on 11 March 2009 and was accepted after revision for publication on 10 November 2009.

DOI: 10.1243/09544070JAUTO1204

Abstract: This paper presents a method for trajectory generation using convex optimization to find a feasible, obstacle-free path for a road vehicle. Consideration of vehicle rotation is shown to be necessary if the trajectory is to avoid obstacles specified in a fixed Earth axis system. The paper establishes that, despite the presence of significant non-linearities, it is possible to articulate the obstacle avoidance problem in a tractable convex form using multiple optimization passes. Finally, it is shown by simulation that an optimal trajectory that accounts for the vehicle's changing velocity throughout the manoeuvre is superior to a previous analytical method that assumes constant speed.

Keywords: obstacle avoidance, trajectory generation, lane change, convex optimization

1 INTRODUCTION

Active safety systems for road vehicles are of growing importance for drivers and regulators alike. Anti-lock braking systems are now common on new cars, and there are proposals in Europe and the United States to require manufacturers of all vehicles to install electronic stability programmes. As vehicle steer-by-wire technology advances, it is appropriate to consider the implementation of automatic obstacle avoidance as an additional active safety system. Longitudinal collision avoidance controllers are starting to appear in luxury vehicles, integrated with forward-looking obstacle detection sensors and cruise control functions to assist the driver when braking. However, these are of limited use for preventing head-on collisions or avoiding obstacles that appear suddenly in front of a moving vehicle. Furthermore, at high speeds an evasive lateral manoeuvre can be performed in a shorter distance than would be required for a vehicle to stop [**1**]. Many drivers habitually risk collision by driving dangerously close to the car in front, and would be unlikely to use driver-aids that prevented them from doing so. It is therefore essential that an emergency collision avoidance system should make use of lateral manoeuvres if it is to be of benefit in most emergency situations. Few studies, however, have explored the use of such aggressive lateral manoeuvres for emergency collision avoidance.

Accordingly, the focus of this paper is on the primary reference trajectory generator and how it might be improved while retaining physical realizability. There are of course many other technologies that must come together to create a full collision avoidance system, including advances in both sensor technology to improve situational awareness and driver–vehicle interface developments to ensure that man and machine operate in harmony. However, this work focuses specifically on trajectory generation, which is independent of the way in which obstacles are detected or decisions to act are made.

Previous work [**2**] developed an automatic lateral collision avoidance system with a particular hierarchical control architecture consisting of reference trajectory generator, feedforward controller, and feedback controller. The most critical part of this control architecture is the reference trajectory generator, which must generate a path that is sufficiently aggressive to avoid obstructions yet can be

**Corresponding author: School of Engineering and Computing, Glasgow Caledonian University, Cowcaddens Road, Glasgow G4 0BA, UK.*
email: geraint.bevan@gcu.ac.uk

tracked feasibly by the feedforward/feedback controller using physically realizable actuation signals under varying vehicle operating conditions.

In reference [**2**], an analytical trajectory generation method is based upon physical and geometrical considerations. However, the method assumes a constant vehicle speed and does not therefore take advantage of speed reductions that could allow the vehicle to turn more sharply during the manoeuvre. Hattori *et al.* [**3**] on the other hand describe an efficient optimal trajectory method but neglect rotation of the vehicle relative to the fixed Earth axis. The current paper demonstrates the importance of including vehicle rotation in the problem formulation. Moreover, it is shown that the obstacle avoidance problem for a rotating vehicle at non-constant speed can be represented in a convex optimization form, and can consequently be solved readily using existing software packages.

The paper is organized as follows. Section 2 describes the choice of axis systems. Section 3 describes the criteria required of a reference trajectory and demonstrates the importance of accounting for vehicle rotation. Section 4 outlines the vehicle equations of motion and the obstacle specification based upon an ISO standard as well as explaining some of the non-linearities inherent in the system. A convex formulation of the obstacle avoidance optimization problem is presented in section 5. Results of applying the method to a specified manoeuvre in vehicle simulations are analysed in section 6. Conclusions are presented in section 7. Finally, a list of the notation used is included in the Appendix.

2 AXIS SYSTEMS

Two axis systems, fixed Earth and vehicle body respectively, are shown in Fig. 1. The vehicle body axis system is a right-hand orthogonal axis set of velocities ($\dot{X}$, $\dot{Y}$) centred on the vehicle centre of mass with $\dot{X}$ defined positive forwards along the centreline of the vehicle and $\dot{Y}$ defined positive to the right of the vehicle. Since this axis system moves with the vehicle, it is not useful for measuring vehicle position relative to the ground. Therefore, a fixed Earth axis system ($X^{\oplus}, Y^{\oplus}$) is defined to be collocated and aligned with the vehicle axis at some point before the start of any manoeuvre, but does not subsequently move with the vehicle. The angle of rotation between these axis systems is the vehicle heading angle, Ψ. Each wheel is labelled, namely, 1, front left; 2, front right; 3, rear left; and 4, rear right.

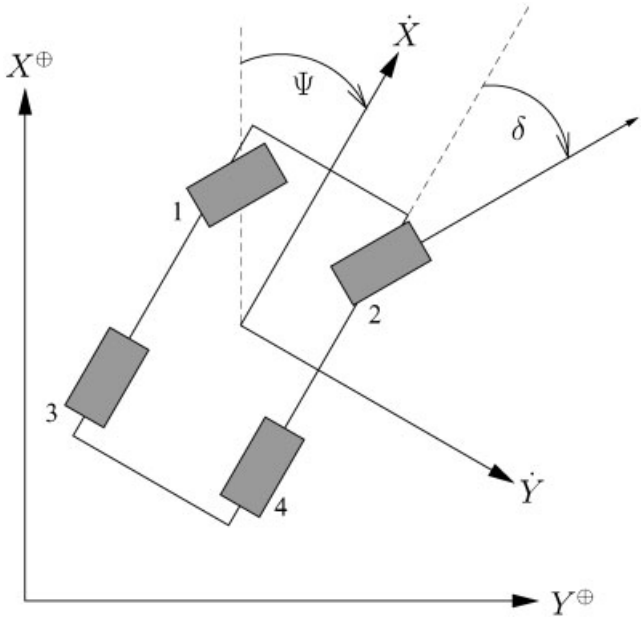

Fig. 1 Fixed Earth and body axis systems

Velocity and acceleration vectors in the vehicle body axis system can be converted into the fixed Earth axis system by rotating the vector through Ψ radians. At time t

$$\dot{X}^{\oplus}(t) = \dot{X}(t)\cos\Psi(t) - \dot{Y}(t)\sin\Psi(t)$$

$$\dot{Y}^{\oplus}(t) = \dot{X}(t)\sin\Psi(t) + \dot{Y}(t)\cos\Psi(t)$$

3 REFERENCE TRAJECTORIES

An architecture for an obstacle avoidance system is shown in Fig. 2. The purpose of an obstacle avoidance system is to cause a vehicle to navigate safely in the presence of obstructions by changing speed and/or steering around them. For a vehicle equipped with brake- and steer-by-wire, this can be achieved by automatic controllers which read measurements from the vehicle sensors and use the data to generate control demands for the actuators: the steering and braking systems. To operate, such feedback controllers require a reference input – a target against which the sensor outputs can be compared.

It is not necessary that the reference trajectory be calculated in real time. Indeed, a more likely implementation would be to generate a series of look-up tables from which the vehicle controller can select according to the conditions detected. Such an approach is consistent with the development of flight control software in the aerospace industry, and

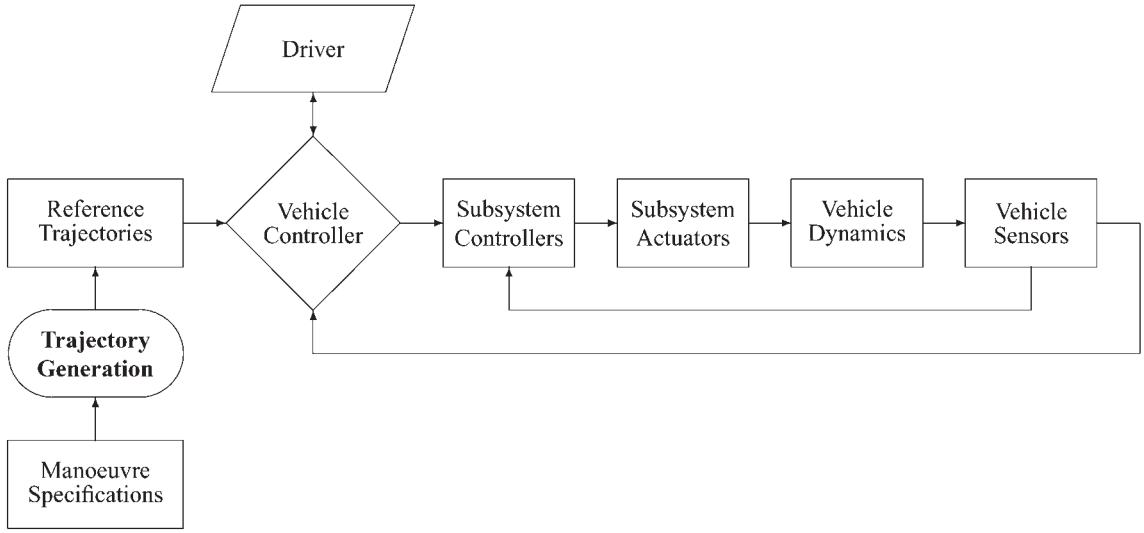

Fig. 2 Architecture for an obstacle avoidance system. Reference trajectories are generated from manoeuvre specifications and loaded into the vehicle controller – a vehicle management system which decides when to act and what strategies to adopt. The selected reference trajectory is compared to sensor data and converted into reference inputs for the subsystem controllers

lends itself readily to comprehensive verification and validation of the control system.

At its simplest, a reference trajectory may consist of a series of instantaneous step changes that reflect the boundary constraints on the vehicle's path. Control systems can be devised that would generate tolerable outputs in such circumstances. However, a reference trajectory that takes little account of a vehicle's dynamic limitations cannot be tracked closely. Controllers attempting to follow such a path must be designed with the expectation of large error values, which precludes the implementation of highly sensitive control throughout the manoeuvre. It has been found previously that developing a good reference trajectory, i.e. one that the vehicle is capable of tracking, reduces the difficulty of designing vehicle controllers [**2**].

3.1 Reference trajectory criteria

A reference generator should have the following attributes. First, it should specify *a priori* the desired reference trajectory according to some criterion in as simple and effective a way as possible. Second, notwithstanding the simplicity of the reference trajectory generation, the resulting controlled vehicle manoeuvre should be feasible. By feasible it is meant that a non-linear vehicle model for varying operating conditions should execute the required lateral manoeuvre under control actions that are physically realizable and not excessive. For verification of feasibility, the non-linear vehicle model itself should not rely on assumptions and approximations inherent in the *a priori* design of the reference trajectory. Instead its greater complexity should validate the specified reference trajectory.

Criteria used in specifying an optimal reference trajectory include minimizing the time or distance of a manoeuvre as demonstrated in the Californian PATH project [**4**]. However, these criteria are not of particular importance if the obstacle to be avoided is in a fixed position or if its position throughout the manoeuvre can be constrained to a definite region. For vehicles seeking to continue travelling at high speed throughout the collision avoidance manoeuvre, perhaps to merge into a new lane without causing a collision with other fast-moving traffic, it may be more appropriate to seek a trajectory that is both smooth and minimizes control effort, so that sufficient control authority is retained for a delegated controller to compensate for disturbances and uncertainties. Sledge and Marshek [**5**] observe that the characteristics of such a trajectory are analogous to the natural bending of a beam. They find a reference trajectory analytically by minimizing the mean-square curvature of the path. However, their solution also relies on the vehicle travelling at constant forward velocity, which precludes the use of brakes and limits the manoeuvre to vehicles travelling below a crtitical speed. Blank and Margolis

[**6**] show that minimizing the path curvature is beneficial for assisting the driver if both steering and braking inputs are saturated, which does account for changing speed but does not encompass the general case.

Note that an optimal solution implies that an objective criterion has been minimized or maximized. A trajectory that is optimal is not necessarily better than one that is not, unless the objective criterion accurately measures the desirability of the outcome. This is not necessarily the case.

For the present work, it is assumed that the vehicle heading remains tangential to the path. Such an assumption places implicit requirements on any controller attempting to track the trajectory. However, it is shown in section 6 that this does not present a problem.

Under the assumption of path tangentiality, in which the yaw rate is locked to path direction, minimizing the instantaneous path curvature for a given speed is equivalent to minimizing the yaw acceleration of the vehicle. As acceleration is proportional to force, this might be expected to yield a smooth desired trajectory that does not waste control effort. Hence the criterion adopted in the current paper for reference trajectory generation is minimization of vehicle yaw acceleration.

Cars routinely travel at high speed in tightly constrained environments. The stopping distance is generally large compared to the dimensions of the vehicle, while the channels in which the car is constrained to remain are usually little wider than the breadth of the vehicle and substantially narrower than its length. Thus the orientation of a car is an integral part of generating a suitable trajectory, and the vehicle dynamics strongly influence the feasibility of following any path.

3.2 The importance of rotation

Hattori *et al.* [**3**] generate an obstacle avoidance trajectory by considering the vehicle as a non-rotating point mass and performing a convex optimization in the vehicle's body axis system. That method neglects yawing of the vehicle and therefore does not take account of rotation of the vehicle axis system relative to the Earth. It is necessary to extend the work if the constraints are specified in the fixed Earth axis system. To illustrate the importance of considering rotation, suppose it is desired that the vehicle follows a trajectory $Y^{\oplus}(t) = \cos(\alpha X^{\oplus}(t)) - 1$, where α is a constant, at constant forward speed u. If the vehicle is considered to be a point mass and rotation of the axis is neglected, the necessary equations of motion would be simply

$$\dot{X}(t) = u, \quad \dot{Y}(t) = -\alpha u \sin(\alpha u t)$$

However, in reality the car would yaw while following such a trajectory. If it is assumed that there is little lateral slip and that the vehicle heading angle is therefore tangential to the direction of motion, i.e. $\Psi(t) = \arctan[(\mathrm{d}Y/\mathrm{d}X)(t)]$, then the velocity in the fixed Earth axis would be

$$\begin{pmatrix} \dot{X}^{\oplus}(t) \\ \dot{Y}^{\oplus}(t) \end{pmatrix} = \mathbf{R}(t) \begin{pmatrix} \dot{X}(t) \\ \dot{Y}(t) \end{pmatrix}$$

where

$$\mathbf{R}(t) = \begin{pmatrix} +\cos\arctan\dfrac{\mathrm{d}Y}{\mathrm{d}X}(t) & -\sin\arctan\dfrac{\mathrm{d}Y}{\mathrm{d}X}(t) \\ +\sin\arctan\dfrac{\mathrm{d}Y}{\mathrm{d}X}(t) & +\cos\arctan\dfrac{\mathrm{d}Y}{\mathrm{d}X}(t) \end{pmatrix}$$

Noting that

$$\sin\arctan\chi \equiv \frac{\chi}{\sqrt{1+\chi^2}} \quad \text{and}$$

$$\cos\arctan\chi \equiv \frac{1}{\sqrt{1+\chi^2}}$$

the rotation matrix becomes

$$\mathbf{R}(t) = \frac{1}{\sqrt{1+(\mathrm{d}Y/\mathrm{d}X)(t)^2}} \begin{pmatrix} +1 & -\dfrac{\mathrm{d}Y}{\mathrm{d}X}(t) \\ +\dfrac{\mathrm{d}Y}{\mathrm{d}X}(t) & +1 \end{pmatrix}$$

The trajectory derivative is $(\mathrm{d}Y/\mathrm{d}X)(t) = -\alpha\sin(\alpha X(t)) = -\alpha\sin(\alpha u t)$ and thus the actual velocity that would be seen in the fixed Earth axis is

$$\dot{X}^{\oplus}(t) = \frac{u\left(1-\alpha^2\sin^2(\alpha u t)\right)}{\sqrt{1+\alpha^2\sin^2(\alpha u t)}}$$

$$\dot{Y}^{\oplus}(t) = \frac{-2u\alpha\sin(\alpha u t)}{\sqrt{1+\alpha^2\sin^2(\alpha u t)}}$$

Figure 3 shows the effect of axis rotation due to yaw on the trajectory: at any point in the manoeuvre, the lateral distance traversed by the vehicle relative to its starting position in the fixed Earth axis would be twice that measured in the vehicle axis system. Clearly, if a trajectory is required to avoid obstacles specified in the fixed Earth axes, this axis rotation

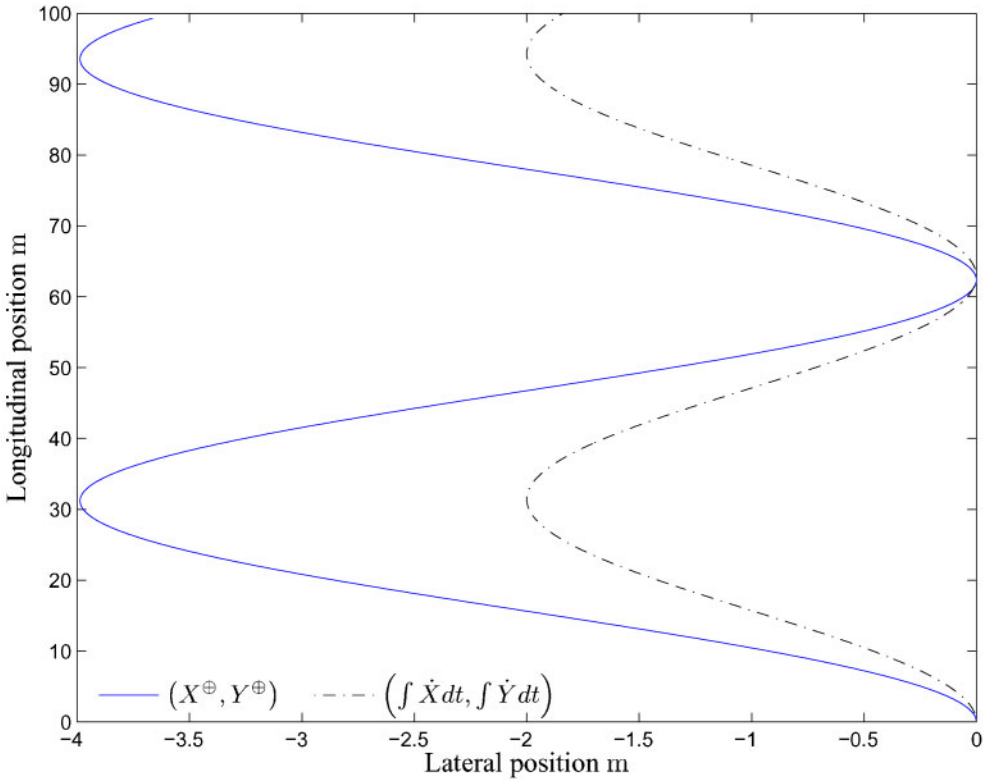

Fig. 3 Effect of axis rotation due to yaw on the trajectory for a vehicle following the trajectory $Y(t) = \cos[\alpha X(t)] - 1$ at forward speed 10 m/s with $\alpha = 0.1$

must be considered during the trajectory generation process.

4 EQUATIONS OF MOTION AND OBSTACLE SPECIFICATION

Richard Hamming said that the purpose of computing is insight, not numbers [**7**]. This applies directly to model development. All models are an abstraction of reality. The appropriate level of abstraction depends on the intended purpose.

Detailed analysis of vehicle performance requires high-fidelity models. Dynamicists often use sophisticated representations of tyre behaviour (e.g. references [**8**] to [**11**]) and account for effects such as load transfer under braking and cornering (e.g. references [**12**] to [**14**]).

Control engineers also make use of models, and good control systems often encompass a description of the dynamics that they are designed to regulate. However, the level of abstraction is usually higher. Feedback mechanisms can account for modelling approximations. Thus control engineers often work with linearizations and other simplifications (e.g. references [**15**] to [**17**]).

The development of reference inputs is one step removed further still. If the aim is to develop a feasible trajectory, i.e. one that the vehicle is capable of tracking accurately, it is necessary to consider the overall constraints on its behaviour. But it is not necessary to consider in detail how those constraints arise or how the control system might follow that trajectory.

The following sections describe the equations of motion and constraints that apply to the vehicle. The resultant model is run repeatedly by an optimization routine, so simplicity is paramount for the sake of computational efficiency.

4.1 Equations of motion

Vehicle dynamics researchers commonly formulate equations of motion in the body axis system (X, Y). As a rotating (i.e. non-inertial) frame, this gives rise to centrifugal terms in the translational equations [**18**], namely

$$m\left(\ddot{X} - \dot{Y}\dot{\Psi}\right) = F_x, \quad m\left(\ddot{Y} + \dot{X}\dot{\Psi}\right) = F_y \tag{1}$$

where m is the vehicle mass and F_x and F_y are the total longitudinal and lateral forces acting on the

vehicle respectively. However, in this work, which is focused on trajectory generation through an obstacle course rather than handling qualities, the interest is primarily in the position and orientation of the vehicle relative to the manoeuvre boundary. Accordingly, the equations of motion are formulated in the fixed Earth (inertial) frame ($X^{\oplus}$, $Y^{\oplus}$), thus

$$m\ddot{X}^{\oplus} = F_{x^{\oplus}}, \quad m\ddot{Y}^{\oplus} = F_{y^{\oplus}} \tag{2}$$

where $F_{x^{\oplus}}$ and $F_{y^{\oplus}}$ are the total forces resolved into components in the inertial frame

$$\begin{pmatrix} F_{x^{\oplus}} \\ F_{y^{\oplus}} \end{pmatrix} = \begin{pmatrix} +\cos\Psi & -\sin\Psi \\ +\sin\Psi & +\cos\Psi \end{pmatrix} \begin{pmatrix} F_x \\ F_y \end{pmatrix} \tag{3}$$

Rotational dynamics are unaffected by the choice of axis ($\dot{\Psi} = \dot{\Psi}^{\oplus}$), hence

$$J_{zz}\ddot{\Psi}^{\oplus} = J_{zz}\ddot{\Psi} = M_z \tag{4}$$

where J_{zz} is the moment of inertia about the vertical axis through the centre of mass and M_z is the corresponding moment.

In the absence of aerodynamic and gravitational forces, all acceleration of the vehicle on a flat road must result from the forces between the tyres and the road. Consideration of the longitudinal $F_{x,j}$ and lateral $F_{y,j}$ contributions of each wheel j to the total forces and moments acting on the vehicle gives rise to expressions for the total forces in the body axis system

$$\begin{aligned} F_x &= \sum_{j=1}^{4} F_{x,j} \\ F_y &= \sum_{j=1}^{4} F_{y,j} \\ M_z &= \sum_{j=1}^{4} l_{x,j}F_{y,j} + l_{y,j}F_{x,j} \end{aligned} \tag{5}$$

where $l_{x,j}$ is the longitudinal moment arm of each wheel and $l_{y,j}$ is the corresponding lateral moment arm.

4.2 Constraints

The forces that can be produced by the tyres are limited by traction saturation. To find a feasible trajectory through an obstacle course, it is necessary to account for this limit, which places bounds on the maximum achievable acceleration.

The magnitude of the longitudinal and lateral forces (relative to the orientation of a wheel) can be described as functions of longitudinal and lateral slip between the tyre and the road. When longitudinal and lateral slip combine, the maximum available force can be estimated by creating a 'friction ellipse' [**19**]. This traction limit will generally be elliptical because tyres can usually generate slightly more traction longitudinally than laterally. Combining the friction ellipses for each wheel gives a friction ellipse for the entire vehicle. This describes the limit of tractive force that can be applied in any direction, given perfect control inputs. Friction ellipses are explained in depth by Milliken and Milliken [**20**].

There are significant difficulties with attempting to form an accurate friction ellipse for a vehicle. Many of the parameters are highly uncertain, dependent on the make and model of tyre, its condition, and that of the road. The friction ellipses for each tyre are also non-linearly dependent on vertical load, which varies as the vehicle pitches and rolls during a manoeuvre, and dependent on the orientation of the wheels relative to the vehicle's velocity vector.

However, it is not necessary to go to this level of detail to find a feasible trajectory. The maximum traction that can be generated by a tyre, irrespective of direction, is determined by the product of the friction coefficient and the load [**21**]. For the vehicle as a whole, it is therefore reasonable to approximate the friction ellipse as a circle of radius μmg N where μ is the maximum friction coefficient between the road and tyres (approximately unity for dry asphalt) and mg is the weight of the vehicle. Resolving the frictional force into components in either the fixed Earth or body axis system yields a constraint on the achievable tyre forces

$$\sqrt{\left(F_x^{\oplus}\right)^2 + \left(F_y^{\oplus}\right)^2} = \sqrt{\left(F_x\right)^2 + \left(F_y\right)^2} \leqslant \mu mg \tag{6}$$

where $g \approx 9.81\,\mathrm{m/s^2}$ is the constant of gravitational acceleration on the Earth's surface. For different operating conditions or surfaces, appropriate scheduled values of μ are substituted into the constraint equation (6).

Assuming that longitudinal forces contribute little to vehicle yaw acceleration – as is the case with the standard bicycle model – the lateral forces will determine the achievable yaw moment. An upper bound on the yawing moment is obtained by assuming that the lateral forces produce a pure couple, acting with moment arm l_f, the distance of the

front axle from the centre of gravity, hence

$$|\ddot{\Psi}| = \frac{|M_z|}{J_{zz}} \leqslant \frac{l_f}{J_{zz}} \sum_{j=1}^{4} |F_{y,j}|$$

For a vehicle travelling straight ahead (small Ψ) with little lateral slip (small $\dot{Y}$), this relationship can be combined with the constraint equation (6) to set a limit for the longitudinal and yaw accelerations relative to the maximum available traction

$$\ddot{\Psi}^2 \leqslant \left(\frac{l_f m}{J_{zz}}\right)^2 \left[(\mu g)^2 - \left(\ddot{X}^{\oplus}\right)^2\right]$$
$$\approx \left(\frac{l_f m}{J_{zz}}\right)^2 \left[(\mu g)^2 - (\ddot{X})^2\right]$$

In addition to the position of the centre of mass, it is also necessary to consider whether any of the wheels will cross any of the boundary lines. Orientation of the vehicle will affect these wheel positions and is particularly important if the channel through which the vehicle must navigate is narrow. The lateral position w_j of each wheel relative to the vehicle centre of mass in the fixed Earth axis is simply

$$w_j = l_{x,j} \sin \Psi + l_{y,j} \cos \Psi$$

The problem of calculating a trajectory constrained by an Earth-fixed boundary is complicated by the presence of significant non-linearities, namely axis rotation, traction saturation, and coupling of control inputs. However, determination of the precise control inputs required to achieve desired accelerations can be delegated to a vehicle dynamics controller once a reference trajectory has been calculated through the obstacle course.

4.3 Obstacle specification

During normal driving scenarios, particularly on multi-lane roads, viable lateral obstacle avoidance will often result in a lane change. International Standard ISO 3888 [**22**] specifies test track layouts for lane-changing manoeuvres. The tests are intended to aid qualitative assessment of vehicle dynamics by experienced drivers, but can serve as a useful objective for evaluating the performance of an automatic vehicle dynamics controller, and hence that of the trajectory planning on which it depends. Two test tracks are described: Part 1 specifies a double lane-change manoeuvre; Part 2 details a similar but more aggressive double lane change, shown in Fig. 4, designed to test emergency obstacle avoidance performance. The latter is more challenging because of its more tightly constrained geometry and is used to demonstrate an optimal trajectory generation method in the sequel. The standard recommends that tests be performed at speeds of 80 ± 3 km/h. Test track dimensions for a vehicle of width 1.57 m are given in Fig. 4.

5 OPTIMAL TRAJECTORY CALCULATION USING NUMERICAL OPTIMIZATION

A non-optimal method of calculating a feasible trajectory to perform the specified manoeuvre is given by Bevan *et al.* [**2**]. The technique makes use of physical principles to identify a good trajectory by assuming a friction circle, calculating a corresponding minimum radius of turn for the vehicle, then building a trajectory from the sharpest possible turns connected by straight lines, thus constructing a geodesic path as espoused by Dubins [**23**]. However, the method does not explicitly consider the reduction in vehicle speed that arises from use of the brakes during the manoeuvre and the consequent relaxation of the yaw rate limit that this affords. There is a natural trade-off within the system of the equations that describe the vehicle dynamics throughout the manoeuvre: use of the brakes reduces the traction available for steering while they operate, thus increasing the instantaneous minimum achievable radius of trajectory curvature, but reduces the future minimum radius of curvature because of the reduction in vehicle speed. The presence of this trade-off suggests that a trajectory can be computed that is optimal in the sense of balancing use of braking against steering. Given the inherent non-linearity and complexity of the system, it is reasonable to seek such an optimal trajectory using numerical optimization.

5.1 Optimization objective

Selection of an appropriate objective is an important part of any optimization. In the introduction, a case is presented for minimizing the instantaneous yaw acceleration of the vehicle throughout the manoeuvre, in order to find a smooth path that does not needlessly waste traction. This can be accomplished by setting the norm of the yaw acceleration vector as the optimization objective to be minimized.

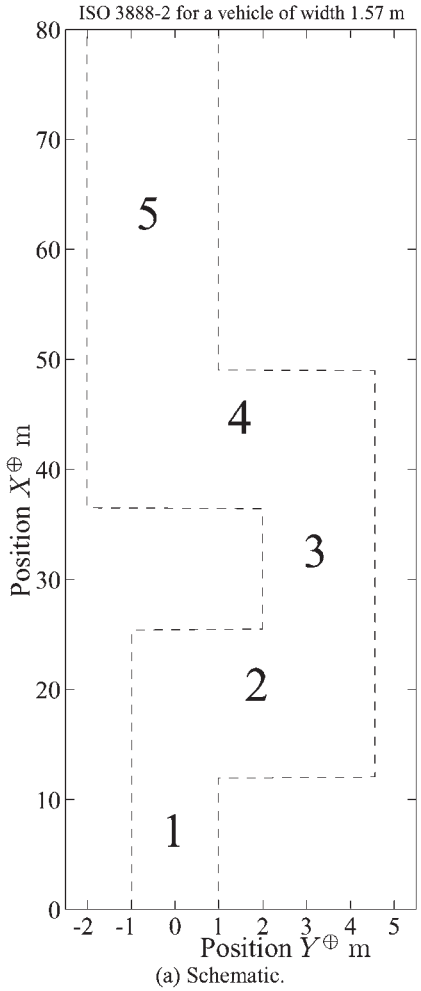

(a) Schematic.

Section	Length (metres)	Width (metres)
1	12.0	1.98
2	13.5	5.55
3	11.0	2.57
4	12.5	6.57
5	12.0	3.00

(b) Dimensions.

Fig. 4 Test track layout and dimensions based upon the layout specified in ISO 3888 Part 2 for a vehicle of width 1.57 m: (a) schematic diagram; (b) dimensions

There are secondary objectives which may be considered to be desirable characteristics of a good trajectory, but which are not explicitly accounted for by the optimization procedure. First, it should be possible to calculate a feasible trajectory that will allow the car to move to safety when travelling at high speed; the higher the initial speed for which a trajectory can be obtained, the greater the usefulness of the method. Recall that a feasible trajectory means one that can be executed by a non-linear vehicle model using control inputs that are physically realizable and not excessive. Second, traction saturation should not be induced unnecessarily so that additional control inputs may be applied to compensate for any deviation of the vehicle from its trajectory. Third, it may be desired that the vehicle should exit the manoeuvre with a forward speed that is either: (a) as low as possible to assist the driver in making an emergency stop; or (b) as high as possible to enable the vehicle to merge safely with other traffic.

5.2 Grid generation in manoeuvre space

A naive optimization strategy might involve repeatedly running a time-based simulation to determine the full vehicle trajectory resulting from potential control strategies. However, it is not desirable for the optimization routine to run a computationally demanding simulation every time its cost function is evaluated. It is better to operate simultaneously on a full description of the entire system. Direct transcription [**24**] offers an appropriate means of representing the full system.

A grid is established, comprising the system states (vehicle position and velocity) at discrete points throughout the manoeuvre space. Numerical integration of the equations of motion is then achieved by converting an appropriate quadrature function into a set of constraints.

The manoeuvre boundary is specified as a function of longitudinal distance in the fixed Earth axis system. It is therefore convenient to generate the

grid with longitudinal distance $X^{\oplus}$ as the independent variable. Choosing any other parameter, such as time, would result in a non-constant set of boundary constraints and a significant increase in computational complexity.

Considering an initial position $X_0^{\oplus}$ and a further set of L points along the $X^{\oplus}$ axis, with equidistant spacing Δ, then the position of the ith point is $X_i^{\oplus} = X_0^{\oplus} + i \times \Delta \forall i \in [0, L]$. The grid $\mathbb{G}$ is then defined as $\mathbb{G} = (\boldsymbol{G}_0, \ldots, \boldsymbol{G}_L) \in \mathbb{R}^{6 \times (L+1)}$ where $\boldsymbol{G}_i = \boldsymbol{G}(X_i^{\oplus})$ $\forall i \in [0, L]$ and $\boldsymbol{G}(X^{\oplus}) = (X^{\oplus}, Y^{\oplus}, \Psi, \dot{X}, \dot{Y}, \dot{\Psi})^{\mathrm{T}} \in \mathbb{R}^6$.

The fully formulated trajectory generation problem is not convex but certain simplifying assumptions enable the formulation of convex approximations to the system of equations. It is thereby possible to take advantage of the power of convex optimization algorithms. The solution is obtained using a series of optimizations, with successively relaxed assumptions, using the CVX [**25**] Matlab package which implements the disciplined convex optimization modelling framework of Grant *et al.* [**26**].

5.3 Optimization problem specification

Objective. The optimization objective is to minimize the yaw acceleration of the vehicle throughout the length of the manoeuvre

$$\text{Minimize } J = \left\| \ddot{\Psi} \right\|$$

Grid spacing. The grid spacing is arbitrarily set to $\Delta = 1\,\text{m}$, a distance which is expected to provide sufficient resolution for the trajectory to take shape without requiring excessive computation.

Initial conditions. The Earth axis is fixed at the starting position of the vehicle, which is initially moving straight ahead with a forward speed of 22.2 m/s (80 km/h) and has no lateral or yaw component of velocity

$$X_0^{\oplus} = 0\,\text{m} \quad Y_0^{\oplus} = 0\,\text{m} \quad \Psi_0 = 0\,\text{rad}$$
$$\dot{X}_0 = 22.2\,\text{m/s} \quad \dot{Y}_0 = 0\,\text{m/s} \quad \dot{\Psi}_0 = 0\,\text{rad/s}$$

Terminal conditions. At the manoeuvre terminus, it is desired that the vehicle should perform lane-keeping and maintain a steady heading along the centre-line of the lane in which it is travelling, which is located approximately half a metre to the right of its initial position

$$Y_L^{\oplus} = -0.5093\,\text{m} \quad \Psi_L = 0\,\text{rad} \quad \dot{\Psi}_L = 0\,\text{rad/s}$$

Quadrature. The vector $\boldsymbol{G}$ is evaluated at each grid point by performing a forward Euler integration with the time T that the vehicle takes to cover the distance between each grid point used as the integration step length

$$\boldsymbol{G}_{i+1} = \boldsymbol{G}_i + \dot{\boldsymbol{G}}_i \times T \quad \forall i \in [0, L]$$

Acceleration limits. Traction saturation, in the form of the nominal friction circle derived in section 4.2, is expressed as a limit on the yaw acceleration. Two further limits are imposed: on the longitudinal velocity, to ensure that the vehicle does not reverse at any time; and on the longitudinal acceleration, to ensure that the vehicle does not increase its speed

$$\dot{X} \geqslant 0 \quad \ddot{X} \leqslant 0 \quad \ddot{\Psi}^2 \leqslant \left(\frac{m l_{\mathrm{f}}}{J_{zz}}\right)^2 \left[(\mu g)^2 - \ddot{X}^2\right]$$

Course boundary. The requirement that the vehicle remain within the defined track is expressed as a constraint on the positions of the wheels, which are limited by a lower boundary $b_l^{\oplus}$ and an upper boundary $b_u^{\oplus}$, representing the left and right hand limits of the track respectively. The vector w_j describes the lateral position of the jth wheel, in the fixed Earth axis system relative to the vehicle centre of mass, and is thus a function of the vehicle orientation

$$b_l^{\oplus} \leqslant Y^{\oplus} + w_j \leqslant b_u^{\oplus} \quad \forall j \in [1, 4]$$

Non-convex constraints. There are several constraints that are incompatible with a convex problem formulation, because they involve trigonometric functions of a vector to be optimized and/or the product or quotient of two such vectors. Various terms in each of the following constraint equations are replaced in each of the optimization runs so that the problem can be specified in a form suitable for solution by a convex algorithm. The problematic constraints are

$$\text{Axis rotation} \quad \begin{cases} \dot{X}^{\oplus} = \dot{X}\cos\Psi - \dot{Y}\sin\Psi \\ \dot{Y}^{\oplus} = \dot{X}\sin\Psi + \dot{Y}\cos\Psi \end{cases}$$

$$\text{Wheel positions} \quad \begin{cases} w_j = l_{x,j}\sin\Psi + l_{y,j}\cos\Psi \\ \forall j \in [1, 4] \end{cases}$$

$$\text{Time step} \quad \begin{cases} T = \frac{\Delta}{\dot{X}^{\oplus}} \end{cases}$$

The integration step length presents a problem if the speed is allowed to vary. The vehicle dynamic equations are expressed as rates in the time domain whereas the grid is specified as a function of distance. If the speed were constant, multiplication by a fixed constant would allow rates to be expressed in terms of distance. However, this is not possible when the speed varies. For quadrature evaluation during the optimization, nominal fixed time steps of length Ts are chosen to represent the time taken for the vehicle to travel between each grid point. Inconsistencies between distance, speed, and time are then reconciled during post-processing.

Axis rotation leads to a set of non-convex constraints owing to the presence of trigonometric terms and the multiplication of vectors. Inclusion of vehicle orientation for determination of wheel positions leads to similar problems. One solution that can often be applied to robotic trajectory planning is to consider a circle of sufficient diameter to enclose the entire vehicle, in which case the orientation does not matter. However, the length of a car is generally significantly longer than its width. In this case, such an encompassing circle would exceed the boundaries, which are defined in terms of the vehicle width. Thus it is necessary to include the vehicle orientation. However, if it is assumed that the vehicle heading angle is small, a first-order Taylor expansion of these trigonometric functions leads to an affine formulation.

In the constraint equations that follow, these non-convex equations are replaced with approximations in which only the vectors denoted with an over-line can vary during the optimization, i.e. $\overline{\dot{X}}$, $\overline{\dot{X}^{\oplus}}$, $\overline{\dot{Y}^{\oplus}}$, $\overline{\Psi}$, and $\overline{w_j}$. All other parameters and vectors are held constant during optimization, but may be altered during post-processing.

5.4 Multi-stage optimization

The optimization is performed in three stages. The overall trajectory generation problem is highly nonlinear and non-convex. By performing the calculation in three stages, it is possible to articulate the constraints using a series of convex approximations. Convex optimization algorithms can then be applied to each representation in turn, leading to a solution to the overall non-convex problem.

To formulate a convex representation, the first stage optimization requires several assumptions and approximations that affect the suitability of the solution. The second and third stages make use of earlier results to relax some of these assumptions, thus enabling closer convergence with the true solution.

5.4.1 First pass

The first pass determines a feasible path, the locus of which has an appropriate shape to respect the boundary constraints and which is attainable within the traction limits of the tyres. Several assumptions and approximations are made to render the system in a convex form. In particular, it is assumed that: the manoeuvre is performed at constant speed; there is no lateral slip; and the heading angle remains small. The resulting trajectory will not obey the boundary limits when mapped into the real fixed Earth axis system, but provides a useful starting point for refinement in subsequent stages.

Having identified an approximate solution, the trajectory is post-processed. The tangent to the trajectory is calculated throughout the manoeuvre to determine the heading angle, still assuming no lateral slip. This heading angle is then used to rotate the velocity vector and calculate the path that the vehicle would actually have followed. This procedure effectively removes the small angle approximation from the result.

Approximations I

$$\begin{aligned}
&\text{Small angle} && \begin{cases} \cos\Psi & \leftarrow 1 \\ \sin\Psi & \leftarrow \Psi \end{cases} \\
&\text{No lateral slip} && \{\ \ddot{Y} \leftarrow 0 \\
&\text{Constant speed} && \begin{cases} \ddot{X} & \leftarrow 0 \\ T & \leftarrow \Delta \Big/ \dot{X}_0^{\oplus} \end{cases}
\end{aligned}$$

Convex constraints I

$$\begin{aligned}
&\text{Axis rotation} && \begin{cases} \dot{X}^{\oplus} = \dot{X}_0 \\ \overline{\dot{Y}^{\oplus}} = \dot{X}_0 \overline{\Psi} \end{cases} \\
&\text{Wheel positions} && \{\ \overline{w_j} = l_{x,j}\overline{\Psi} + l_{y,j} \qquad \forall j \in [1,4]
\end{aligned}$$

Post-processing I: Following the optimization, the vehicle position at each point is re-evaluated using the calculated heading angle Ψ_{I} instead of the small angle approximation

$$X_{\mathrm{I},i}^{\oplus} \leftarrow X_0^{\oplus} + \int_0^{t_i} \dot{X}_{\mathrm{I}} \cos\Psi_{\mathrm{I}} - \dot{Y}_{\mathrm{I}} \sin\Psi_{\mathrm{I}}\, \mathrm{d}t \qquad \forall i \in [0, L]$$

$$Y_{\mathrm{I},i}^{\oplus} \leftarrow Y_0^{\oplus} + \int_0^{t_i} \dot{X}_{\mathrm{I}} \sin\Psi_{\mathrm{I}} + \dot{Y}_{\mathrm{I}} \cos\Psi_{\mathrm{I}}\, \mathrm{d}t \qquad \forall i \in [0, L]$$

where the subscript I denotes the final values following completion of the optimization and $t_i = i \times T$ denotes the time at which each grid point i is

reached. The heading profile is then rescaled so that it corresponds to the specified grid positions $X_i^{\oplus}$ rather than the longitudinal positions $X_{\mathrm{I},i}^{\oplus}$ actually attained by the vehicle at each point

$$\Psi_{\mathrm{I}}\left(X_i^{\oplus}\right) \leftarrow \Psi_{\mathrm{I}}\left(X_{\mathrm{I},i}^{\oplus}\right) \qquad \forall i \in [0, L]$$

5.4.2 Second pass

A second optimization then allows the speed to vary, holding constant the yaw acceleration profile, as a function of longitudinal distance, under the assumption that the shape of the optimal trajectory will be similar to that found in the first optimization pass. During this second optimization, it is assumed that the longitudinal position at each time coincides precisely with the initial grid spacing. Thus it is assumed that the vehicle covers a distance Δ in each integration step no matter what its velocity.

By pre-calculating $\cos\Psi_{\mathrm{I}}$ and $\sin\Psi_{\mathrm{I}}$ using the heading profile Ψ_{I} from the preceding optimization, it is possible to introduce these trigonometric expressions into the constraint equations as constants, allowing an affine/convex formulation of the vehicle trajectory in the fixed Earth axis system and partially dispensing with the small heading angle approximation.

Approximations II

$$\text{Small angle} \quad \left\{\begin{array}{ll}\cos\Psi & \leftarrow 1\\ \sin\Psi & \leftarrow \Psi\end{array}\right\}\text{for axis rotation}$$

$$\text{Fixed heading profile} \quad \left\{\begin{array}{ll}\cos\Psi & \leftarrow \cos\Psi_{\mathrm{I}}\\ \sin\Psi & \leftarrow \cos\Psi_{\mathrm{I}}\end{array}\right\}\text{for wheel positions}$$

$$\text{No lateral slip} \quad \{\ddot{Y} \leftarrow 0$$

$$\text{Constant speed} \quad \left\{\begin{array}{ll}T & \leftarrow \Delta \big/ \dot{X}_0^{\oplus}\\ \dot{X} & \leftarrow \dot{X}_0\end{array}\right\}\text{for axis rotation } \left(\dot{Y}^{\oplus} \text{ only}\right)$$

Convex constraints II

$$\text{Axis rotation} \quad \left\{\begin{array}{ll}\overline{\dot{X}^{\oplus}} & = \overline{\dot{X}}\\ \overline{\dot{Y}^{\oplus}} & = \dot{X}_0 \overline{\Psi}\end{array}\right.$$

$$\text{Wheel positions} \quad \{w_j = l_{x,j}\sin\Psi_{\mathrm{I}} + l_{y,j}\cos\Psi_{\mathrm{I}} \quad \forall j \in [1, 4]$$

Post-processing II: Following the second optimization, the resulting velocity profile is used to calculate the true longitudinal position of the vehicle at each instant. Reduction in vehicle speed during the manoeuvre reduces the distance covered at each instant. Consequently, it is expected that the vehicle path will impinge on the boundary constraints because the car turns too early. The trajectory is therefore re-calibrated (stretched) to compensate for this deficiency.

The actual vehicle position at each instant is calculated

$$X_{\mathrm{II},i}^{\oplus} \leftarrow X_0^{\oplus} + \int_0^{t_i} \dot{X}_{\mathrm{II}}\cos\Psi_{\mathrm{II}} - \dot{Y}_{\mathrm{II}}\sin\Psi_{\mathrm{II}}\,\mathrm{d}t \qquad \forall i \in [0, L]$$

$$Y_{\mathrm{II},i}^{\oplus} \leftarrow Y_0^{\oplus} + \int_0^{t_i} \dot{X}_{\mathrm{II}}\sin\Psi_{\mathrm{II}} + \dot{Y}_{\mathrm{II}}\cos\Psi_{\mathrm{II}}\,\mathrm{d}t \qquad \forall i \in [0, L]$$

and the heading angle profile is re-calibrated to match the specified grid positions

$$\Psi_{\mathrm{II}}\left(X_i^{\oplus}\right) \leftarrow \Psi_{\mathrm{II}}\left(X_{\mathrm{II},i}^{\oplus}\right) \qquad \forall i \in [0, L]$$

The subscript II here indicates the values obtained from the second pass.

5.4.3 Third pass

A third optimization pass is then performed. As before, the values from the previous run can be used to insert non-convex expressions into the problem specification by holding them constant. In this final optimization, the heading angle (from the previous step) is included in the calculation of longitudinal position. The longitudinal velocity profile of the previous (re-calibrated) trajectory is also used when calculating lateral position, instead of assuming that the vehicle remains at its initial speed. The result of this pass corresponds closely with the vehicle's behaviour in the fixed Earth axis and is the solution sought.

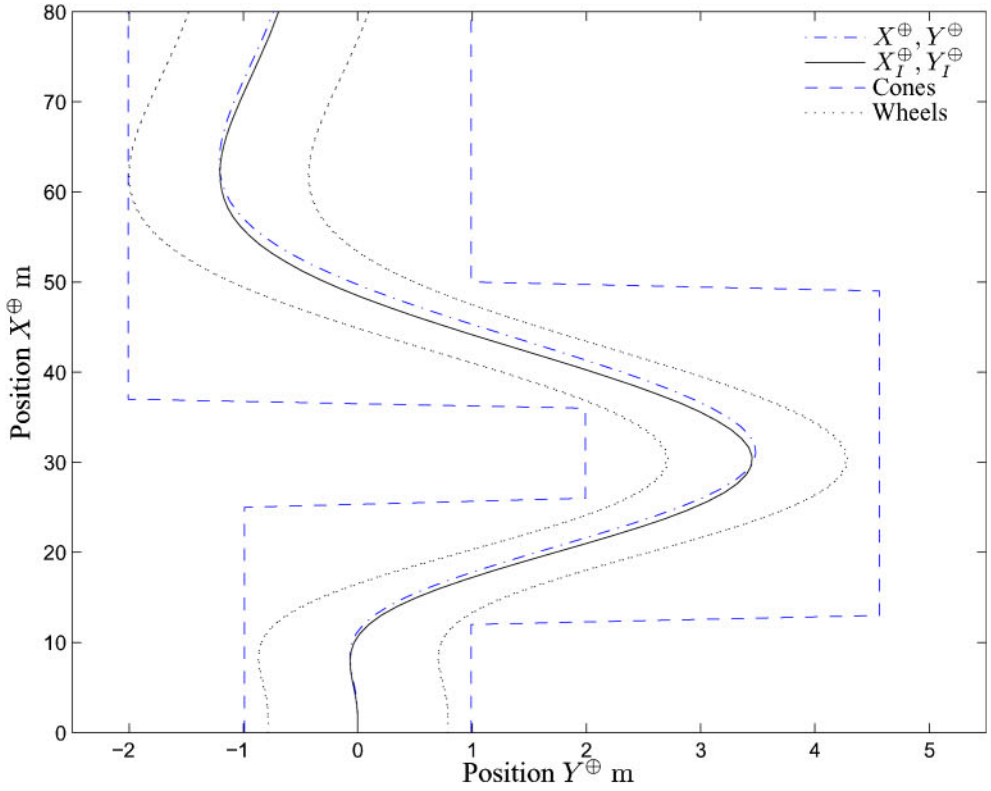

(a) First pass optimisation.

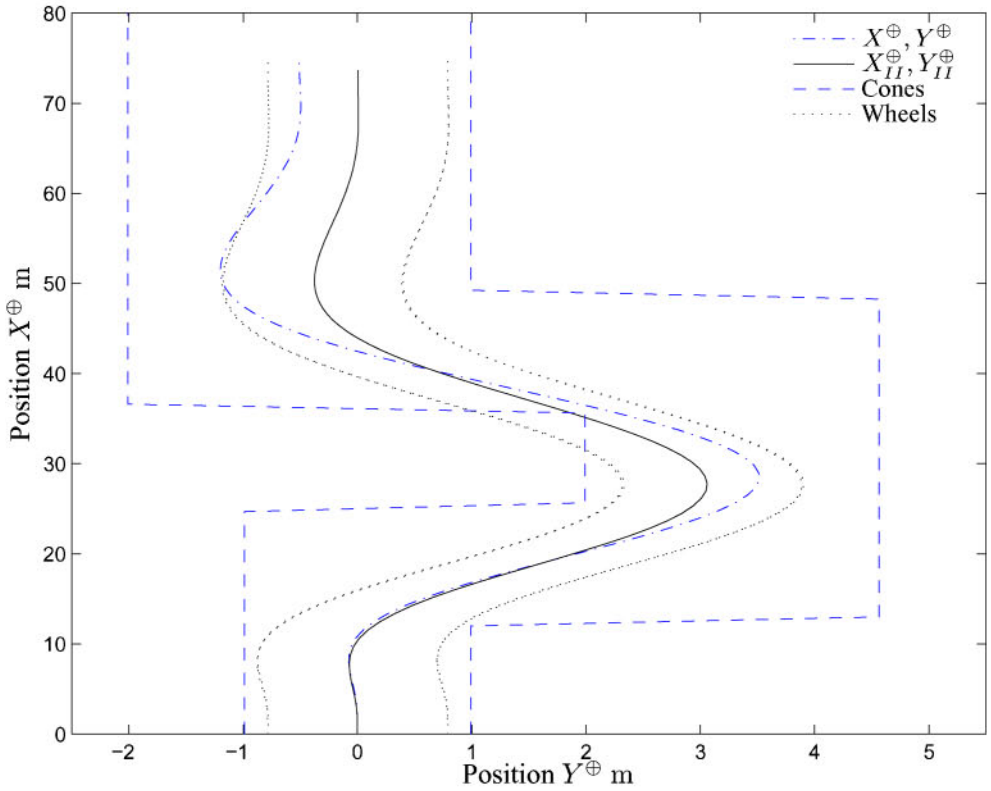

(b) Second pass optimisation.

Fig. 5 Optimization results. The chained lines show the trajectory produced during the optimization. The solid lines show corrections to the trajectory after post-processing using the best available data. Dotted lines indicate wheel positions after post-processing

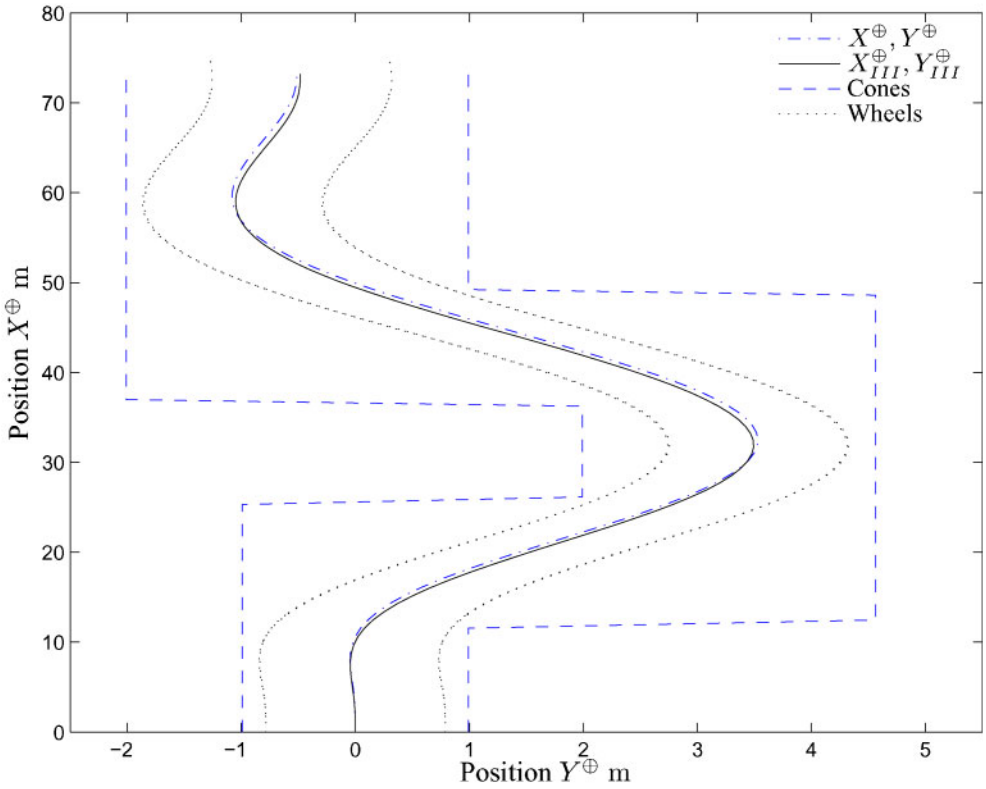

(c) Third pass optimisation.

Fig. 5 (continued)

Approximations III

$$\text{Small angle} \quad \{\sin\Psi \leftarrow \Psi \} \text{ for axis rotation}$$

$$\text{Fixed heading profile} \quad \left\{ \begin{array}{ll} \cos\Psi & \leftarrow \cos\Psi_{\text{II}} \\ \sin\Psi & \leftarrow \sin\Psi_{\text{II}} \end{array} \right\} \text{for wheel positions}$$

$$\text{No lateral slip} \quad \{\ddot{Y} \leftarrow 0$$

$$\text{Constant speed} \quad \left\{ \begin{array}{ll} T & \leftarrow \Delta \big/ \dot{X}_0^{\oplus} \\ \dot{X} & \leftarrow \dot{X}_{\text{II}} \end{array} \right\} \text{for axis rotation} \left(\dot{Y}^{\oplus} \text{ only}\right)$$

Convex constraints III

$$\text{Axis rotation} \quad \left\{ \begin{array}{ll} \overline{\dot{X}^{\oplus}} & = \overline{\dot{X}} \cos\Psi_{\text{II}} \\ \overline{\dot{Y}^{\oplus}} & = \dot{X}_{\text{II}} \overline{\Psi} \end{array} \right.$$

$$\text{Wheel positions} \quad \{w_j = l_{x,j} \sin\Psi_{\text{II}} + l_{y,j} \cos\Psi_{\text{II}} \quad \forall j \in [1,4]$$

6 RESULTS AND DISCUSSION

Figure 5 shows the evolution of the trajectory as the optimization procedure runs through each of the three stages. Figure 5(a) shows that the first pass optimization successfully determines a trajectory that remains within the specified boundaries. However, it should be noted that this trajectory is dependent upon the assumptions under which it was calculated. In particular, it is assumed that the forward speed remains constant.

In Fig. 5(b), it can be seen that the second optimization pass successfully manages to replicate the shape of the manoeuvre from the first pass while accounting for variation in speed. However, the effect of speed reduction, neglected in the first pass, can be clearly seen: a manoeuvre that would have avoided the boundaries at constant speed does in

fact cross the boundary when the speed change is taken into account because the vehicle starts its second lane change too early.

After the trajectory has been re-calibrated to account for the change in speed, the third pass successfully achieves a trajectory that respects the limits, while relying on fewer assumptions. The trajectory is shown in Fig. 5(c).

The trajectory optimization method does not make use of a specific vehicle model. The method was evaluated by simulation using a non-linear two-track model of a passenger vehicle's longitudinal and lateral dynamics, as described in reference [**2**], together with a controller similar to those described by Bevan and co-workers [**2**, **27**], acting on the brakes and front wheel steering. The model is of a luxury passenger car equipped with front-wheel steer-by-wire and brake-by-wire on each wheel, and represents longitudinal and lateral acceleration and the pitch, roll, and yaw dynamics of an unsprung body. Its steering system operates with a rate limit of ± 160 rad/s and is subject to a communication delay of up to 40 ms. The braking system has rate limits of +500 and -2000 bar/s and a communication delay of up to 20 ms. Tyre forces are modelled using the 'magic formula' of Pacejka and Bakker [**8**]. The controller integrates braking and steering commands which act on measurements of lateral position, yaw angle, and yaw rate.

It should be noted that the simulation model does not rely on the assumptions and approximations that were used to design the reference trajectory. Successful execution of the manoeuvres therefore demonstrates the validity of the approximations used for this application. The feasibility of the trajectory is seen in the simulation outputs in Figs 6, 7, and 8, which show the vehicle trajectory, vehicle velocity, and controller outputs.

Figure 6 shows clearly that the wheels remain within the boundary throughout the manoeuvre. The effect of braking can be seen in Fig. 7 as the speed of the vehicle reduces from 80 km/h at the start of the manoeuvre to a final speed of just under 70 km/h. A clear correlation is evident between the lateral velocity and the yaw rate of the vehicle, and the lateral velocity remains small for the entire time, thus justifying the assumption that lateral slip could be neglected. The control inputs from the controller are shown in Fig. 8, which shows that, despite the severity of the manoeuvre, the steering angle remains feasible and the brake forces do not saturate.

An important assumption in the problem formulation was that the vehicle heading angle remains tangential to the direction of motion. The validity of this assumption can be seen in Fig. 9, which shows the tangent of the heading angle Ψ in comparison with the trajectory tangent $\mathrm{d}Y^{\oplus}/\mathrm{d}X^{\oplus}$.

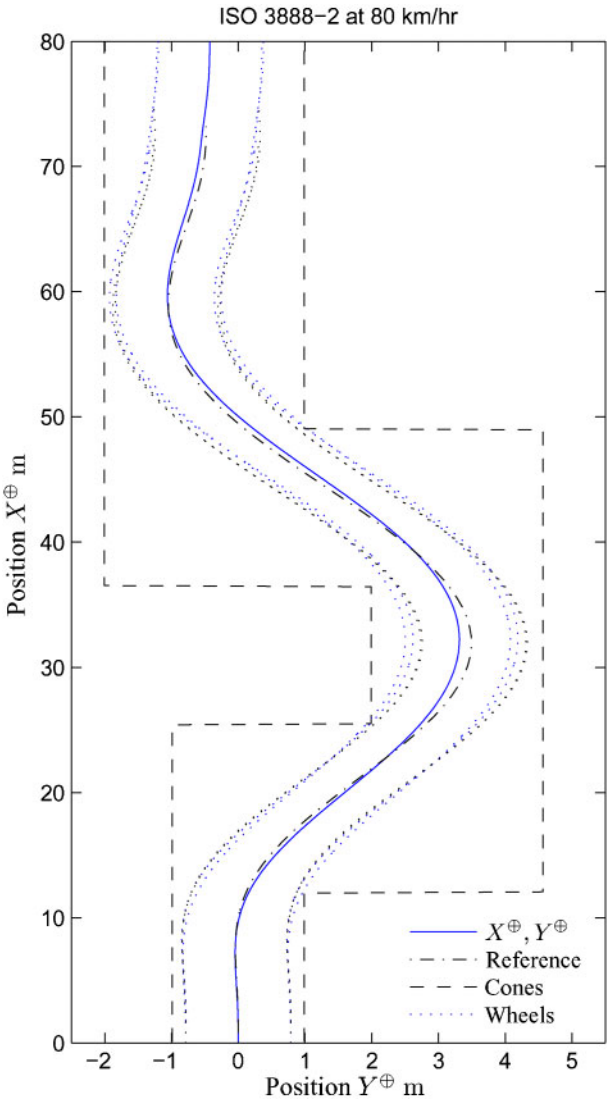

Fig. 6 Output trajectory for a double lane change manoeuvre with initial speed $\dot{X}_0 = 80$ km/h

6.1 Comparison with a non-optimal generation method

The three-stage trajectory optimization procedure outlined above was applied to calculate a trajectory with a higher initial speed of 90 km/h. The result can be seen in Fig. 10 alongside a corresponding trajectory calculated using the method of Bevan *et al.* [**2**]. In both cases, a trajectory is calculated that can be followed by a simulated vehicle when driven by an appropriate controller. However, a limitation is evident in the non-optimal reference trajectory;

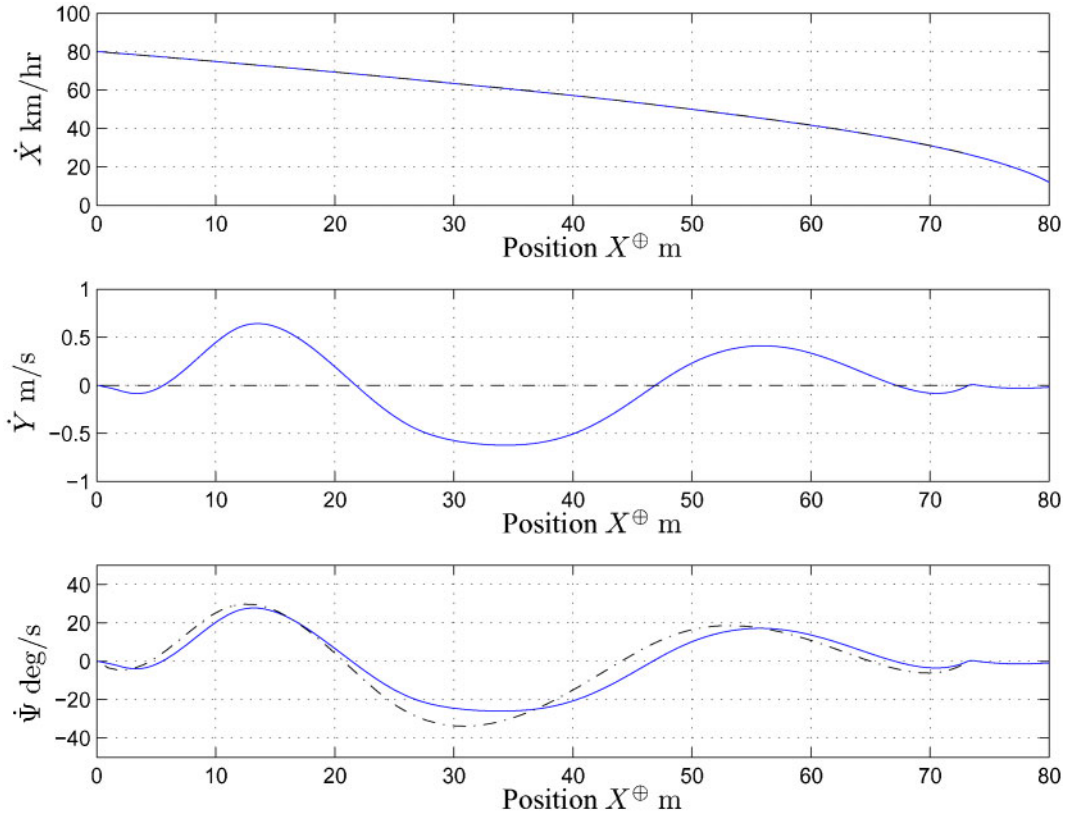

Fig. 7 Longitudinal, lateral, and yaw velocities for a double lane change with initial speed $\dot{X}_0 = 80\,\text{km/h}$

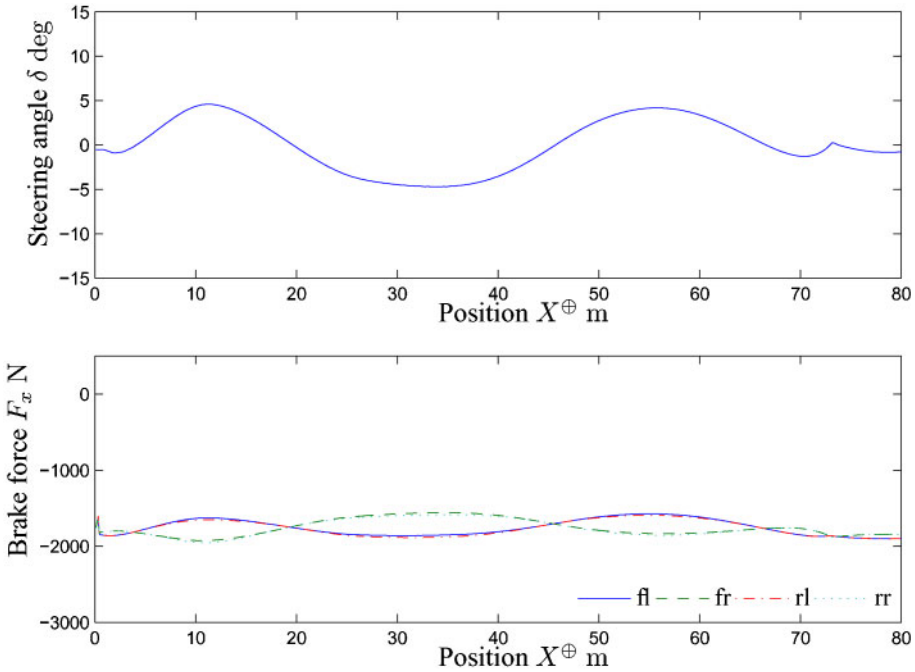

Fig. 8 Control inputs, steering δ, and brake forces F_x on the front left, front right, rear left, and rear right wheels for a double lane change manoeuvre with initial speed $\dot{X}_0 = 80\,\text{km/h}$

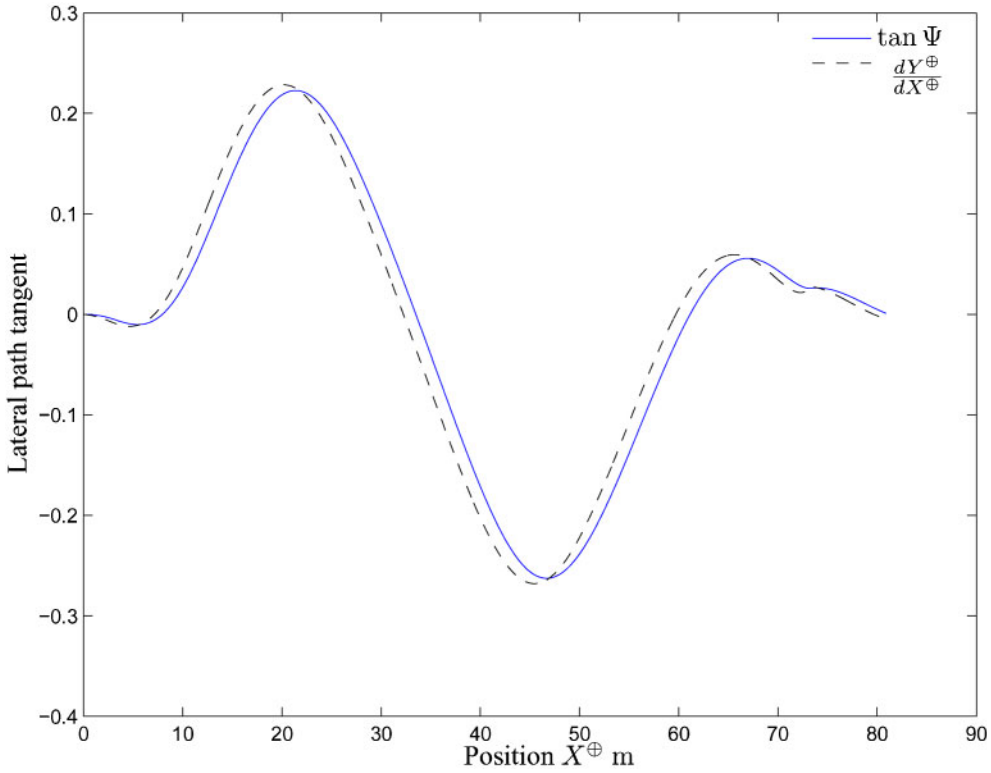

Fig. 9 Validation of heading angle assumption

it can be seen that there is a discontinuity at $X^{\oplus} \approx 30$ m. This discontinuity is the result of overlapping circles of minimum turning radius. Furthermore, the non-optimal trajectory results in the first corner being cut slightly. The simulation shows that the vehicle is still able to complete the remainder of the manoeuvre, but that is only because the operation of the brakes causes the vehicle to slow, thus reducing the minimum achievable radius of curvature. However, this effect is not accounted for in that trajectory generation. In contrast, the optimal trajectory explicitly accommodates the changing speed and therefore generates a smooth trajectory that avoids the boundary throughout the entire manoeuvre.

The superiority of the optimal method is also evident at the start of the manoeuvre where it can be seen that the optimal trajectory initially turns away from the intended direction, allowing more room for the vehicle to avoid clipping the first corner.

The optimal trajectory method aims to minimize the norm of the yaw acceleration throughout the manoeuvre. It would therefore be expected that the yaw acceleration exhibited while using the optimal trajectory would be less than that resulting from the non-optimal method. Figure 11 shows that this is indeed the case, whether the manoeuvre is performed at 80 or 90 km/h.

7 CONCLUSIONS

This paper presents a method for trajectory optimization to achieve road vehicle obstacle avoidance using convex optimization. It builds upon recent work on collision avoidance by automatic emergency lateral manoeuvre where the hierarchical control architecture consists of reference trajectory generator, feedforward controller, and feedback controller. The results of the paper concentrate on the most critical part of this control architecture, the reference trajectory generator, which must generate an optimal vehicle trajectory that is sufficiently aggressive yet feasible for the feedforward/feedback controller. More details of the resultant superior feedforward/feedback controller performance for a severe lane change derived from an ISO standard are reported elsewhere [**28**].

There are three main conclusions. First, it is shown that, despite the presence of significant nonlinearities, it is possible to articulate the obstacle avoidance problem in a convex form if the optimiza-

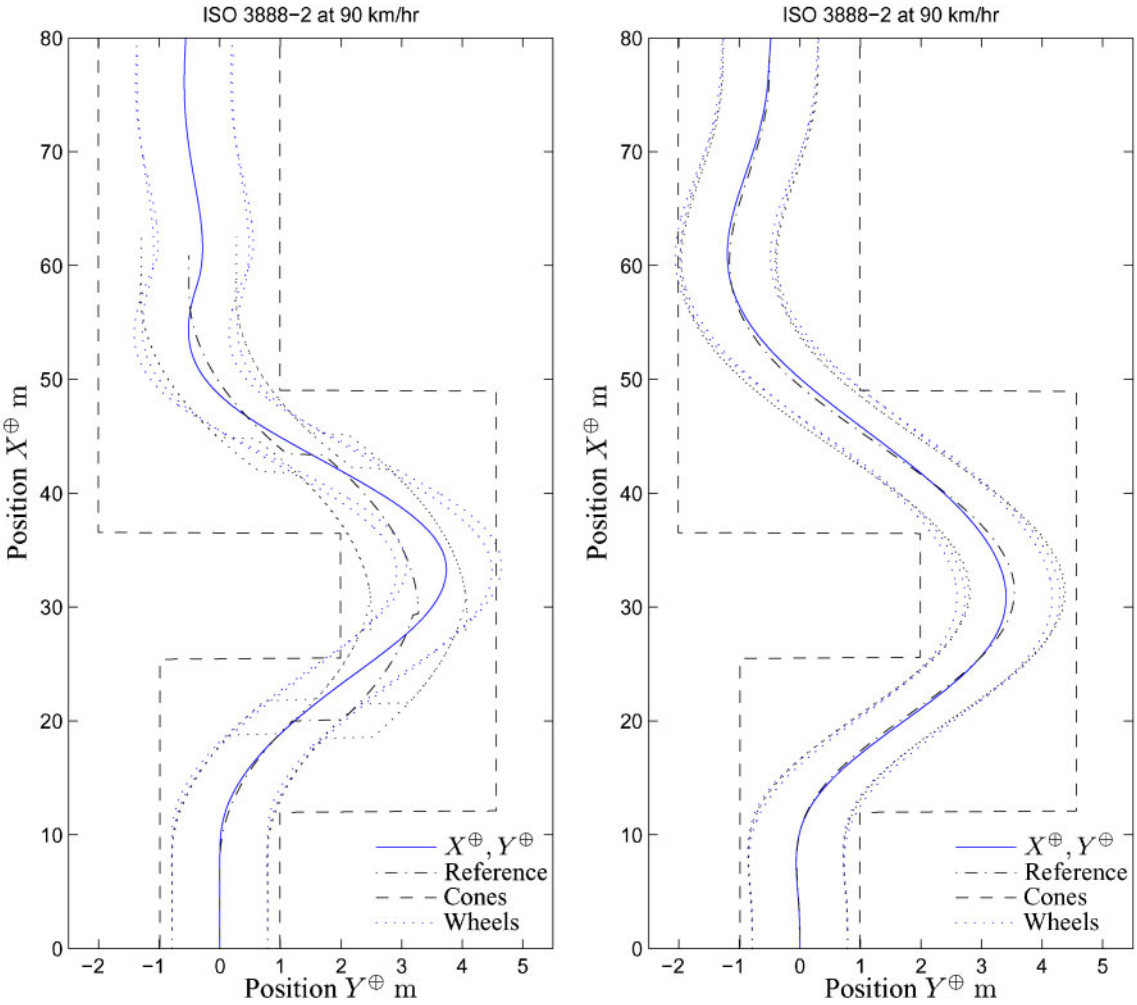

(a) Trajectory using method of Bevan *et al.*[2]. (b) Optimal trajectory.

Fig. 10 Simulation results: reference and output trajectory ($\dot{X}_0 = 90$ km/h). It can be seen that the non-optimal reference (a) is not feasible. It has discontinuities at approximately 20, 30, and 45 m and the wheels cut the corner of the boundary at 25 m. Contradistinctively, the optimal trajectory (b) is smooth and the simulated vehicle follows it successfully, remaining within the specified limits

tion is allowed to converge to a solution over multiple passes. Specifying the problem in this way offers access to powerful and efficient numerical solvers that can take advantage of this convexity.

Second, it is necessary to consider rotation of the vehicle relative to the fixed Earth axis if the reference trajectory is required to avoid obstacles specified in this axis system. It has been shown that, for even a simple periodic trajectory, the lateral displacement of the vehicle may be twice that which would be indicated if axis rotation is neglected.

Finally, it is demonstrated that an optimal trajectory that accounts for the vehicle's changing velocity throughout the manoeuvre is superior to a previous analytical method that assumes constant speed. The procedure can generate a trajectory at higher vehicle speeds than would otherwise be possible.

Global convergence is not guaranteed. The optimal trajectory generation technique outlined in this paper has been successfully applied to several other single and double lane-change vehicle manoeuvres, which are not presented here. In all cases investigated so far, three optimization passes have been sufficient to ensure convergence of the optimal trajectory. In future work, it is likely that feasible problems could be devised, which require subsequent passes or which entirely fail to converge due to numerical instability. It would be of interest to identify necessary and sufficient conditions to guarantee convergence. In particular, it is expected that

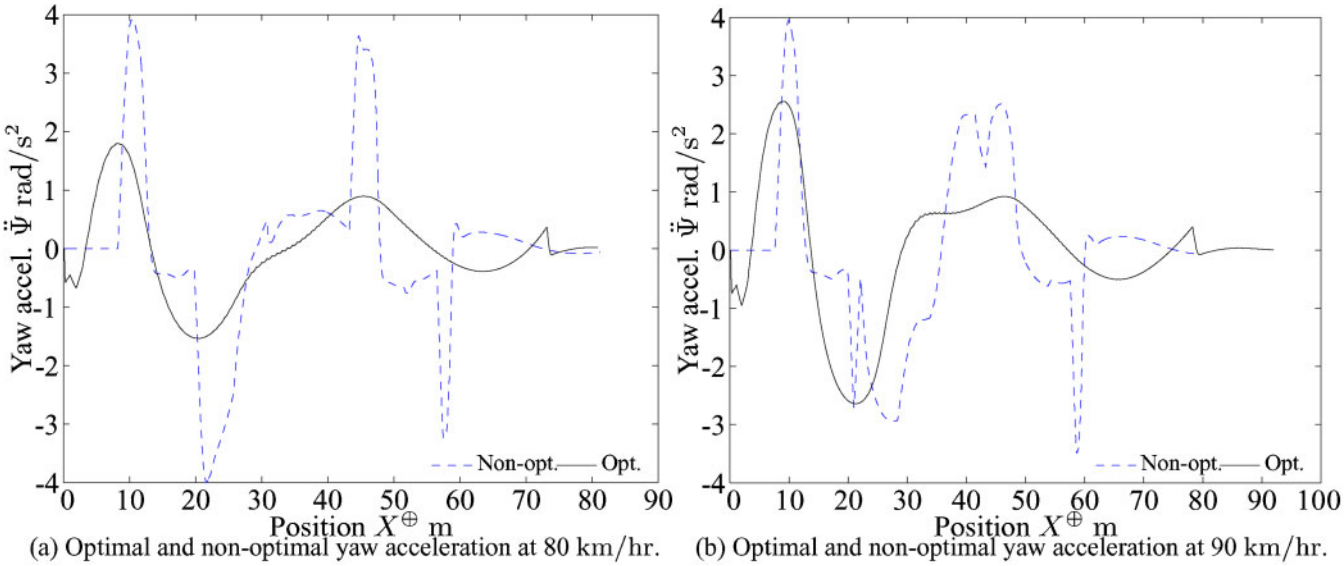

Fig. 11 Yaw acceleration at 80 and 90 km/h. At 80 km/h, the optimal and non-optimal methods both produce feasible reference trajectories. It is seen that a controller following the non-optimal trajectory requires higher yaw accelerations. At 90 km/h, only the optimal trajectory is feasible. Again, the yaw acceleration tends to be lower

altering the grid spacing Δ, and hence the number of grid points L, would affect the performance of the trajectory optimization procedure.

ACKNOWLEDGEMENTS

This research was supported by the EU Sixth Framework Programme specific targeted research project Complex Embedded Automotive Control Systems (CEmACS) under contract 004175. The authors wish to thank Daimler Research, and in particular Dr Jens Kalkkuhl, for invaluable assistance with this work. The opinions expressed in this paper are, however, solely those of the authors.

REFERENCES

1 **Shiller, Z.** and **Sundar, S.** Emergency lane-change manoeuvres of autonomous vehicles. *Trans. ASME, J. Dynamic Systems, Measmt Control*, 1998, **120**, 37–44.

2 **Bevan, G. P., Gollee, H.,** and **O'Reilly, J.** Automatic lateral emergency collision avoidance for a passenger car, *Int. J. Control*, 2007, **80**(11), 1751–1762.

3 **Hattori, Y., Ono, E.,** and **Hosoe, S.** Optimum vehicle trajectory control for obstacle avoidance problem. *IEEE/ASME Trans. Mechatronics*, 2006, **11**, 507–512.

4 **Godbole, D. N., Hagenmeyer, V., Sengupta, R.,** and **Swaroop, D.** Design of emergency maneuvers for automated highway system: obstacle avoidance problem. In Proceedings of the IEEE Conference on *Decision and control*, San Diego, California, December 1997, vol. 5, pp. 4774–4779 (Institute of Electrical and Electronics Engineers, London).

5 **Sledge Jr, N. H.** and **Marshek, K. M.** Development and validation of an optimized emergency lane-change trajectory. In *Vehicle dynamics and simulation*, Detroit, Michigan, February 1998, no. 1361, pp. 103–121 (Society of Automotive Engineers, Warrendale, Pennsylvania).

6 **Blank, M.** and **Margolis, D. L.** Minimizing the path radius of curvature for collision avoidance. *Veh. System Dynamics*, 2000, **33**(3), 183–201.

7 **Hamming, R. W.** *Numerical methods for scientists and engineers,* 2nd edition, 1973 (McGraw-Hill).

8 **Pacejka, H. B.** and **Bakker, E.** The magic formula tyre model. *Veh. System Dynamics*, 1993, **21**, 1–18.

9 **Canudas de Wit, C.** and **Tsiotras, P.** Dynamic tire friction models for vehicle traction control. In Proceedings of the IEEE Conference on *Decision and control*, Phoenix, Arizona, December 1999, vol. 4, pp. 3746–3751 (Institute of Electrical and Electronics Engineers, London).

10 **Gäfvert, M.** and **Svendenius, J.** Construction of novel semi-empirical tire models for combined braking and cornering. Technical Report ISRN LUTFD2/TFRT–7606–SE, Department of Automatic Control, Lund Institute of Technology, Sweden, April 2003.

11 **Pauwelussen, J. P., Gootjes, L., Schröder, C., Köhne, K. U., Jansen, S.,** and **Schmeitz, A.** Full vehicle ABS braking using the SWIFT rigid ring tyre model. *Control Engng Practice*, 2003, **11**, 199–207.

12 **Gissinger, G. L., Chamaillard, Y.,** and **Stemmelen, T.** Modelling a motor vehicle and its braking

system. *Math. Computers in Simulation*, 1995, **39**, 541–548.

13 **Ammon, D., Gipser, M., Rauh, J.,** and **Wimmer, J.** High performance system dynamics simulation of the entire system tire–suspension–steering–vehicle. *Veh. System Dynamics*, 1997, **27**, 435–455.

14 **Jansen, S. T. H., Zegelaar, P. W. A.,** and **Pacejka, H. B.** The influence of in-plane tyre dynamics on ABS braking of a quarter vehicle model. *Veh. System Dynamics*, 1999, **32**, 249–261.

15 **Johansen, T. A., Hunt, K. J., Gawthrop, P. J.,** and **Fritz, H.** Off-equilibrium linearisation and design of gain scheduled control with application to vehicle speed control. *Control Engng Practice*, 1998, **6**, 167–180.

16 **Leith, D. J.** and **Leithead, W. E.** Gain-scheduled and nonlinear systems: dynamic analysis by velocity-based linearization families. *Int. J. Control*, 1998, **70**, 289–317.

17 **Burgio, G.** and **Zegelaar, P.** Integrated vehicle control using steering and brakes. *Int. J. Control*, 2006, **79**, 534–541.

18 **Wong, J. Y.** *Theory of ground vehicles*, 3rd edition, 2001 (Wiley, Chichester).

19 **Sharp, R. S.** and **Bettella, M.** On the construction of a general numerical tyre shear force model from limited data. *Proc. IMechE, Part D: J. Automobile Engineering*, 2003, **217**(3), 165–172. DOI: 10.1243/09544070360550363.

20 **Milliken, W. F.** and **Milliken, D. L.** *Race car vehicle dynamics*, 1995 (Society of Automotive Engineers, Warrendale, Pennsylvania).

21 **Gillespie, T. D.** *Fundamentals of vehicle dynamics*, 1992 (Society of Automotive Engineers, Warrendale, Pennsylvania).

22 ISO 3888: *Passenger cars – test track for a severe lane-change manoeuvre*, 1999, 2002 (International Organization for Standardization).

23 **Dubins, L. E.** On curves of minimal length with a constraint on average curvature, and with prescribed initial and terminal positions and tangents. *Am. J. Math.*, 1957, **79**, 497–516.

24 **Betts, J. T.** *Practical methods for optimal control using nonlinear programming*, 2001 (SIAM, Philadelphia).

25 **Grant, M.** and **Boyd, S.** CVX, A Matlab package for disciplined convex programming, 2005. Available from http://www.stanford.edu/~boyd/cvx/ for further details.

26 **Grant, M., Boyd, S.,** and **Ye, Y.** Disciplined convex programming. In *Global optimization: from theory to implementation (nonconvex optimization and its applications)*, 2006, pp. 155–210 (Springer Science and Business Media, New York).

27 **Bevan, G. P.** *Development of vehicle dynamics controller for obstacle avoidance*. PhD Thesis, University of Glasgow, 2008.

28 **Bevan, G. P., O'Neill, S. J., Gollee, H.,** and **O'Reilly, J.** Performance comparison of collision avoidance controller designs. In Proceedings of 2007 IEEE Intelligent Vehicles Symposium, Istanbul, Turkey, June 2007, pp. 468–473 (Institute of Electrical and Electronics Engineers, London).

APPENDIX

Notation

F	force (N)
g	gravitational acceleration (m/s^2)
$\boldsymbol{G}$	grid slice
$\mathbb{G}$	grid
i	grid index
j	wheel index
J	moment of inertia (kg m^2)
l	moment arm (m)
L	number of grid points
m	mass (kg)
M	moment (N m)
$\mathbf{R}$	rotation matrix
t	time (s)
u	forward speed (m/s)
w	wheel lateral position (m)
X	longitudinal distance (m)
Y	lateral distance (m)
α	trajectory parameter
Δ	grid spacing (m)
μ	friction coefficient
χ	generic variable
Ψ	heading angle (rad)

Subscripts and superscripts

j	wheel number
o	initial
T	transpose
x	longitudinal
y	lateral
z	vertical
$\oplus$	Earth axis
I	first iteration
II	second iteration
III	third iteration